EXPERIMENTAL CELL RESEARCH 322 (2014) 265–276

Available online at www.sciencedirect.com

ScienceDirect

journal homepage: www.elsevier.com/locate/yexcr

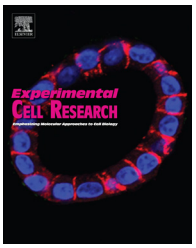

Research Article

Myosin 1e is a component of the invadosome core that contributes to regulation of invadosome dynamics

*Jessica L. Ouderkirk, Mira Krendel**

Cell and Developmental Biology, SUNY Upstate Medical University, 750 E. Adams Street, Syracuse, NY 13210, United States

ARTICLE INFORMATION

Article Chronology:
Received 22 June 2013
Received in revised form
9 January 2014
Accepted 15 January 2014
Available online 22 January 2014

Keywords:
Actin
Myosin
Invadosome

ABSTRACT

Myosin 1e (myo1e) is an actin-based motor protein that has been implicated in cell adhesion and migration. We examined the role of myo1e in invadosomes, actin-rich adhesion structures that are important for degradation and invasion of the extracellular matrix. RSV-transformed BHK-21 cells, which readily form invadosomes and invadosome rosettes, were used as the experimental model. Myo1e localization to the actin-rich core of invadosomes required the proline-rich Tail Homology 2 (TH2) domain. During invadosome rosette expansion, we observed myo1e recruitment to newly forming invadosomes via Tail Homology 1 (TH1)-dependent interactions with the plasma membrane, where it preceded actin and paxillin. Dominant-negative inhibition of myo1e resulted in mislocalized invadosome formation, usually at the center of the rosette. We propose that TH2 domain of myo1e provides the key signal for localization to invadosomes, while TH1 domain interactions facilitate myo1e targeting to the plasma membrane-proximal locations within the rosettes. Myo1e may then act as a scaffold, linking the plasma membrane with the actin cytoskeleton and helping direct new invadosome formation to the periphery of the rosette.

Introduction

Myosin 1e (myo1e) is an actin-dependent molecular motor broadly expressed in vertebrate tissues. Myo1e belongs to myosin class I, which includes several single-headed myosin motors that interact with both actin filaments and membranes/vesicles [1]. Class I myosins consist of a single heavy chain and one or more calmodulin-like light chains. Myo1e heavy chain includes an N-terminal motor or head domain, responsible for actin binding, a neck domain that contains a single IQ motif for binding to light chains, and a C-terminal tail domain. Most class I myosins have tails that consist of a single domain known as TH1 (Tail Homology 1). TH1 domains are rich in positively charged amino acids and bind to acidic phospholipids, promoting myosin localization to the plasma membrane. Myo1e and a closely related myosin, myo1f, form a distinct subclass of class I myosins, known as long-tailed myosins I. These proteins contain two additional domains in their tails: a proline-rich TH2 domain and a C-terminal SH3 domain also referred to as TH3.

The functional roles previously identified for myo1e include involvement in clathrin-mediated endocytosis [2,3], maintenance of normal glomerular filtration in the kidney [4,5], and regulation of cell–cell adhesion [6]. Myo1f, the only other member of long-tailed myosin I subclass in vertebrates, has previously been shown

Abbreviations: BHK, Baby Hamster Kidney cells; FRAP, fluorescence recovery after photobleaching; Myo1e, m1e, myosin 1e; N-WASP, Neural Wiskott Aldrich Syndrome protein; RSV, Rous sarcoma virus; TH, Tail Homology domain; WIP, WASP interacting protein

*Corresponding author.
E-mail address: krendelm@upstate.edu (M. Krendel).

0014-4827/$ - see front matter © 2014 Elsevier Inc. All rights reserved.
http://dx.doi.org/10.1016/j.yexcr.2014.01.015

to play an important role in regulating cell-substrate adhesion and cell migration in neutrophils via modulation of integrin exocytosis [7]. These findings suggest that vertebrate long-tailed class I myosins contribute to a variety of actin-dependent processes. Intriguingly, myo1e has been detected as a component of integrin adhesion complexes in a large-scale proteomic study [8], suggesting that, similarly to myo1f, it may be involved in regulation of cell–substrate adhesion. Since myo1e role in cell–substrate adhesion has not been characterized, we set out to examine its localization and functions in cell-substrate contacts.

Initial observation of myo1e localization in several cell lines showed that it was not highly enriched in focal adhesions or focal complexes. However, we found that myo1e was highly concentrated in podosomes/invadopodia, specialized sites of cell-substrate attachment involved in matrix degradation and invasion [9–11]. Therefore, we focused on characterization of myo1e role in podosomes/invadopodia to determine how it contributes to cell adhesion, using Rous sarcoma virus (RSV)-transformed BHK-21 cells as a model system. BHK-21 is a fibroblast cell line derived from Syrian hamster kidneys and widely used to study virus replication. RSV-transformed BHK-21 cells form numerous invadopodia-like structures arranged in clusters or ring-shaped aggregates [12]. Tyrosine kinase Src, and, in particular, the active form of Src contributed by the RSV v-src gene, plays a key role in assembly of invadopodia. Although invadopodia-like structures formed by RSV-transformed BHK-21 cells are often referred to as podosomes in the literature, in this manuscript we will refer to them as "invadosomes", using a more general term to describe these invasive structures.

Invadosomes are actin-rich adhesion structures containing a dense meshwork of actin filaments at their center, or core, and a ring of adhesion adapter proteins, such as paxillin and vinculin, at their periphery [13,14]. Invadopodia play an important role in tumor cell invasion, representing the site of intense matrix degradation by tumor cells [15–17]. Invadosomes in RSV-transformed cells frequently form superstructures, or rosettes, consisting of multiple invadosomes. Treatment with the tyrosine phosphatase inhibitor sodium orthovanadate, or vanadate, has been shown to accelerate formation of new invadosomes and promote expansion of the rosettes towards the cell periphery [18], resulting in formation of large invadosome rings, similar to podosome belts in osteoclasts. The rosettes expand due to the assembly of new invadosomes at the periphery of the rosette and paxillin-regulated disassembly of invadosomes along the internal rim [18]. The dynamics of invadosome rosette expansion is reminiscent of the process that results in formation of podosome belts in osteoclasts, where new podosomes are assembled along the outer edge of a podosome cluster [19]. Observing rosette expansion in this model allows direct visualization of invadosome dynamics, allowing us to examine the sequence of protein recruitment to the sites of new invadosome assembly at the periphery.

In this study, we used RSV-transformed BHK-21 cells as a model for invadosome dynamics and assembly. We examined localization of myo1e in individual invadosomes and invadosome rosettes. Next, we mapped the domains of myo1e necessary for localization to invadosomes. Finally, we inspected myo1e localization within expanding invadosome rosettes relative to other invadosome markers and analyzed myo1e role in expansion of invadosome rosettes following vanadate treatment.

Materials and methods

Cells, plasmids, antibodies and reagents

RSV-transformed BHK-21 cells were a generous gift from the De Camilli lab, Yale University [20]. Cells were maintained in DMEM with 10% fetal bovine serum (FBS) in 5% CO_2 atmosphere at 37 °C.

All GFP-tagged human myo1e constructs were cloned into pEGFP-C1 vector (Clontech Laboratories, Inc., Mountain View, CA). Cloning of the myo1e full-length and tail constructs was previously described [2]. Domain deletion mutants of myo1e were made by inserting mutations using QuikChange Lightning site-directed mutagenesis kit (Agilent, Santa Clara, CA) or by In-fusion cloning (Clontech Laboratories, Inc., Mountain View, CA). Primers used to subclone TH1 domain surround AA717-921, TH2 domain – AA921-1056, TH3 domain – AA1051-1108. Murine myo1e-mApple [21] was provided by Dr. Christien Merrifield via Addgene (Cambridge, MA).

Monoclonal antibody against paxillin was purchased from BD Transduction Laboratories (Franklin Lakes, NJ). Anti-myo1e polyclonal antibody was previously described [22]. Gelatin was purchased from Sigma (St. Louis, MO) and prepared as previously described [23]. Sodium orthovanadate was purchased from Sigma (St. Louis, MO) and prepared as a 200 μM solution. The solution was activated as previously described [24] and stored at −20 °C. Prior to use, the 200 μM sodium orthovanadate was heated in a 55 °C water bath for 10 min and diluted in DMEM with 10% FBS to a final concentration of 5 μM.

Live cell imaging and immunostaining

RSV-transformed BHK-21 cells (60,000 cells/dish) were plated in 35 mm glass bottom dishes (MatTek Corportaion, Ashland, MA) 48 h prior to imaging. Cells were transfected with 2 μg of DNA plasmid per dish using Jet PEI reagent (Polyplus-Transfection Inc., Illkirch, France) 24 h before imaging. Cells were incubated at 37 °C in medium containing 5 μM activated vanadate for 10 min prior to imaging and during imaging. Cells were plated on 18 mm round glass coverslips 24 h before staining. Prior to staining, cells were treated for 25 min with 5 μM sodium orthovanadate at 37 °C. The staining protocol was similar to the previously described protocols [4,18]. In brief, cells were fixed in 4% paraformaldehyde for 10 min, permeabilized using 0.25% Triton X-100 and blocked in 3% Bovine Serum Albumin in PBS. This was followed by a one-hour incubation with primary antibody and a thirty-minute incubation with a secondary antibody.

To compare the probability of rosette formation in cells expressing either full-length myo1e or myo1e tail construct, cells transfected with the GFP-tagged myo1e constructs were treated with vanadate for 15 min, fixed, and stained with phalloidin. All cells expressing GFP-tagged proteins were counted and scored for the presence or absence of an invadosome rosette. A total of 1300 cells (from approximately 4 22×22 mm^2 coverslips) was scored for each construct. As a control, the number of rosette-forming cells among 1300 untransfected, vanadate-treated cells was also determined. Data are represented as percentages.

All imaging was performed using Perkin Elmer UltraView VoX Spinning Disk Confocal system mounted on a Nikon Eclipse Ti

microscope and equipped with a 100× objective and an environmental chamber to maintain cells at 36 °C.

Image analysis

All image analysis was performed using ImageJ. Line scans of fluorescence intensity were generated using a linear selection (1–20 pixels wide, as indicated in the figure legends) and a "plot profile" function in ImageJ to obtain intensity values for each pixel along the line. When using selections wider than 1 pixel, ImageJ generated mean intensity value for all pixels with the same *x*-position.

For rosette dynamics analysis, following stimulation with vanadate, cells were imaged every 20 s over a 7 min time period. During the subsequent analysis of the time-lapse movies, the behavior of each cell/rosette was categorized under one of four categories: fast expansion, slow expansion, steady state and collapse. For full-length myo1e expressing cells, we used an *n* of 31 cells. For myo1e tail expressing cells, we used an *n* of 21 cells, as finding rosettes in these cells was much more difficult. Data are presented based on percentages.

FRAP analysis

Fluorescence recovery after photobleaching (FRAP) was performed using Perkin Elmer UltraView VoX Spinning Disk Confocal system equipped with the Photokinesis module. Cells were plated in 35 mm glass bottom dishes, transfected, and treated with vanadate at 5 uM concentration. Photobleaching using full power of a 488 nm argon laser was performed by selecting a square region of interest corresponding to a portion of the invadosome rosette, with 15 passes of the laser over the region of interest. Post-bleach images were collected every 0.1 s. Changes in fluorescence intensity in the bleached areas were measured over time and normalized relative to the background and a control region of interest (to correct for acquisition bleaching). The best fit curve for fluorescence recovery was obtained using Kaleidagraph software. The following equation was used: $y=a(1-e^{-bx})$, where x is time in seconds. The half time of recovery was determined using b from the previous equation, where $t_{1/2}=\ln 0.5/-b$. Analysis was performed on 16-bit images. For the full-length myo1e and TH2 constructs, the data represents the average of 5 rosettes analyzed, while TH1TH2 was analyzed in 4 cells. Since fluorescence recovery for the TH2 domain was very rapid, with significant amount of fluorescence recovering within 0.1 s, the measurements for the TH2 construct may slightly underestimate the rate of recovery for this construct.

Results

Myo1e localizes to the actin-rich core of invadosomes

Invadosomes, consisting of an actin core surrounded by a ring of paxillin, were observed in RSV-transformed BHK-21 cells plated on glass coverslips (Fig. 1A). Cell staining with the anti-myo1e antibody revealed colocalization of myo1e with actin at the core of invadosomes (Fig. 1B). Myo1e at the core of invadosomes was surrounded by a ring of paxillin (Fig. 1C). To confirm that these structures were functional, matrix degrading invadosomes, cells were plated on FITC-labeled gelatin and stained with either phalloidin or anti-myo1e antibody (Fig. 1D and E). We observed colocalization of both actin and myo1e with the sites of gelatin degradation. Thus, myo1e localizes to invadosomes in RSV-transformed BHK-21 cells, specifically to the actin-rich core of these structures.

The TH2 domain of myo1e is necessary and sufficient for myo1e localization to invadosomes

To identify the regions of myo1e that are important for localization to individual invadosomes and invadosome clusters, we constructed a variety of GFP-tagged truncation mutants of myo1e (Fig. 2E). We utilized mCherry-tagged Lifeact, a peptide derived from yeast actin binding protein ABP140 [25], to label actin in live RSV-transformed BHK-21 cells. Confocal images of live cells expressing GFP-tagged constructs together with Lifeact were collected. Expression of GFP alone was used as a negative control, showing minimal enrichment at the actin-rich invadosomes (Fig. 2A). As a positive control, a full-length myo1e (GFP-FL myo1e) construct was coexpressed with Lifeact and exhibited localization to invadosomes and invadosome clusters (Fig. 2B). Further experiments showed that the tail of myo1e also localized to invadosomes, indicating that the tail domain is sufficient for myo1e localization to invadosomes (Fig. 2E and Supplementary Fig. 1A). To identify specific regions within the myo1e tail that may target it to invadosomes via protein–protein interactions, we examined localization of deletion mutants of full-length myo1e lacking either SH3 or TH2 domains (Fig. 2E and Supplementary Fig. 1). SH3 domain deletion had no effect on myo1e localization to invadosomes (Fig. 2E and Supplementary Fig. 1D). Myo1e construct lacking TH2 showed greatly diminished localization at invadosome clusters (Fig. 2C) and individual invadosomes, indicating that the TH2 domain is necessary for invadosomal localization of myo1e. When the TH2 domain of myo1e was expressed as a GFP-tagged construct, it localized to invadosome clusters (Fig. 2D), indicating that the TH2 domain is sufficient for myo1e localization to invadosomes. These results are shown graphically in Fig. 2E, where the enrichment of each construct at invadosomes relative to its expression in the cytoplasm was determined by calculating the ratio of the mean fluorescence intensity at invadosome clusters to the mean fluorescence intensity in the cytoplasm (method adapted from [26]).

Myo1e localizes to newly forming invadosomes at the leading edge of expanding invadosome rosettes, and precedes recruitment of actin and paxillin

Treatment of BHK cells with tyrosine phosphatase inhibitor vanadate enhances protein tyrosine phosphorylation and invadosome formation [27]. This treatment promotes clustering of invadosomes into large metastructures called rosettes, as well as the outward expansion of the rosettes [18]. Rosette expansion occurs through formation of new invadosomes at the periphery and disassembly of older invadosomes at the inner rim of the rosette. This expansion of rosettes can be used as a model for analysis of the factors influencing invadosome dynamics, since both assembly and disassembly of invadosomes are enhanced by vanadate treatment. We can also visualize the sequence of events that occurs as new invadosomes form at the periphery.

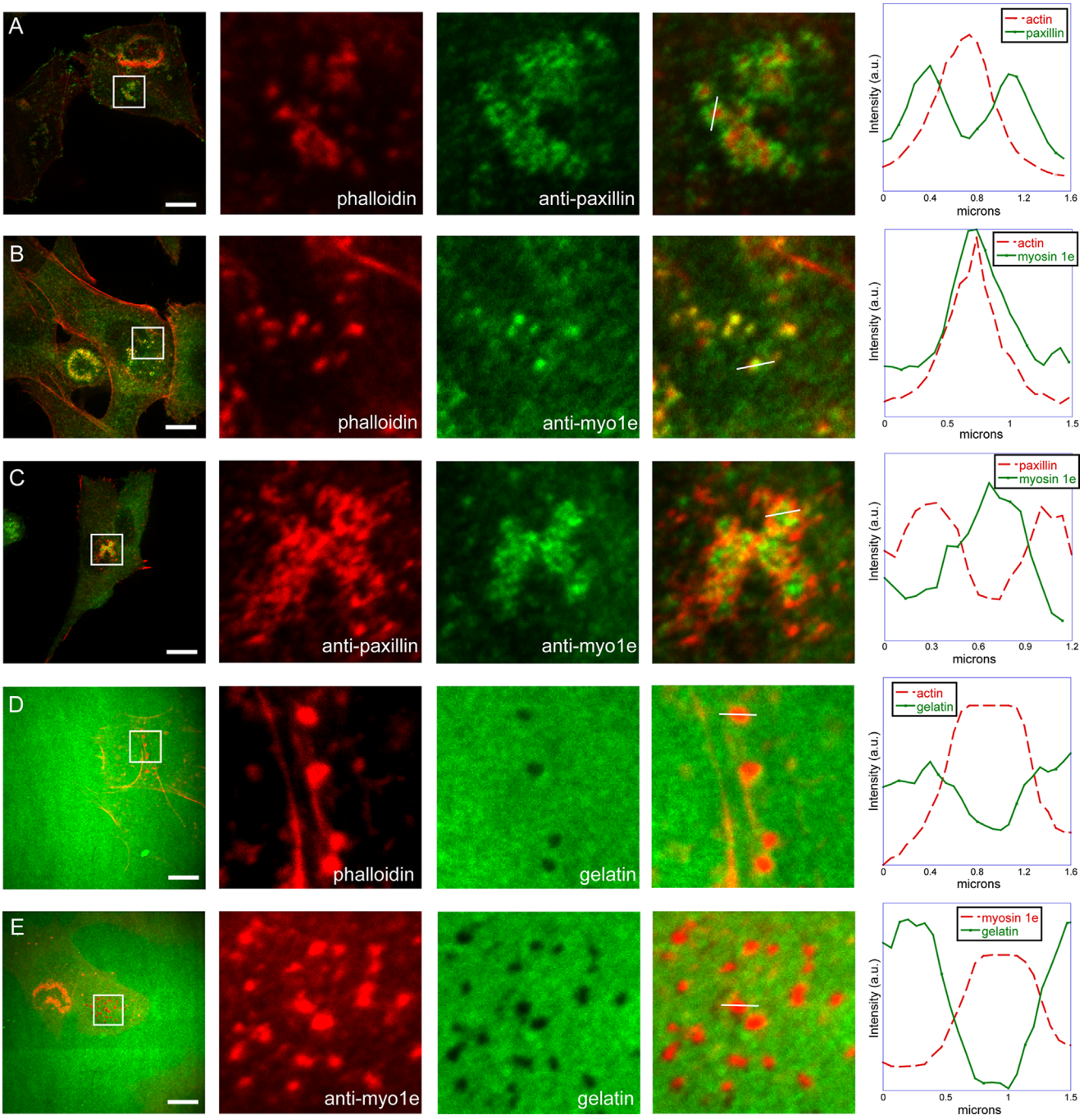

Fig. 1 – Myo1e localizes to the core of invadosomes in RSV-transformed BHK-21 cells. (A) Localization of invadosome components in RSV-transformed BHK-21 cells. Cells were stained with the anti-paxillin antibody and actin filament marker phalloidin. Invadosomes have a characteristic organization, with an actin-rich core surrounded by a ring of paxillin. Most cells contain both individual invadosome and invadosome clusters; for clarity, cell regions containing individual invadosomes were used to analyze the relative localization of invadosome components. (B) Localization of myo1e compared to actin. Antibody-stained myo1e colocalized with actin in the invadosome core. (C) Myo1e localization compared to paxillin. Bright central dot of myo1e is seen surrounded by a ring of paxillin. (D) Cells were plated on fluorescent gelatin for 45 min and fixed. Actin-rich invadosomes, stained with phalloidin, were colocalized with the areas of matrix degradation. (E) Myo1e colocalization with the areas of degradation on fluorescent gelatin. In figures A–E, each inset shows invadosomes in a 10 by 10 μm square. The line through an individual invadosome represents the selection (1 pixel wide) used to measure relative fluorescence intensities that were plotted on the right. Scale bars, 10 μm.

Invadosome expansion can be observed in as little as 5 min following vanadate application and can be visualized by time-lapse imaging of cells expressing fluorescently-tagged Lifeact to label actin (Fig. 3A). Analysis of myo1e localization relative to actin in an expanding invadosome rosette indicated that myo1e was localized closer to the periphery of the rosettes than actin, so

that a ring of GFP-myo1e was visible outside of the ring of mCherry-Lifeact (Fig. 3B). Previously published data shows that paxillin localizes to the inner rim of the rosette and is important for disassembly of older invadosomes [18]. Consistent with this, myo1e was also localized more peripherally than paxillin, as observed in fixed cells stained with anti-paxillin and anti-myo1e antibodies (Fig. 3C). Since the outer rim of the expanding rosette corresponds to the site of formation of new invadosomes [18], we hypothesized that the peripheral localization of myo1e indicated that myo1e recruitment preceded actin assembly during formation of new invadosomes. The peripheral localization of myo1e was observed using either GFP- or mApple-tagged myo1e constructs, indicating that it was independent of the order of collection of fluorescence images (red channel was always collected first).

Using confocal microscopy, we examined the expanding invadosome rosette structure in three dimensions (Fig. 3D–G). We observed a difference in myo1e localization at the bottom surface of the rosette, where the rosette makes contact with the substrate, and the top of the rosette, which is in closer proximity to the cell body (Fig. 3D–E). At the bottom surface of the rosette, myo1e localization appeared more uniform throughout the rosette (Fig. 3D). At the top of the rosette, myo1e was preferentially localized to the outer surface of the expanding rosette (Fig. 3E). This localization corresponded to a cup-shaped distribution of myo1e fluorescence intensity observed in a 3-D reconstruction of the rosette (Fig. 3F–G), where myo1e appeared to surround actin and localize to the ventral surface and sides of the invadosome rosette. These observations suggest that myo1e may be enriched in the plasma-membrane-proximal areas within the expanding invadosome rosette. Based on these observations, subsequent imaging of truncated myo1e constructs (Fig. 4) was performed by collecting Z-sections through the middle portion of the rosette, which was characterized by the most pronounced gradient of myo1e distribution.

Localization of myo1e to the periphery of expanding invadosome rosettes requires TH1-dependent interactions with the plasma membrane

As described above, myo1e localization in expanding invadosome rosettes was characterized by high concentration along the membrane-bound outer rim of the rosettes and a somewhat lower concentration inside the rosettes. The enrichment of myo1e along the outer edge of the rosettes was also observed using immunostaining of endogenous myo1e in vanadate-treated cells (Fig. 4A), indicating that the distribution of myo1e across the rosette was not a byproduct of overexpression of GFP-myo1e.

This distinct distribution was observed in cells expressing both the full-length myo1e and the tail domain of myo1e, suggesting that some of the domains comprising myo1e tail contribute to this localization (Fig. 4A–C). When the TH2 domain was expressed alone, it exhibited a uniform distribution throughout the expanding rosette, without any enrichment along the plasma membrane, suggesting that although the TH2 domain is necessary for localization to invadosomes, it is not sufficient for the appropriate localization of myo1e to newly forming invadosomes within an expanding rosette (Fig. 4D). Myo1e construct containing the TH1 and TH2 domains demonstrated the non-uniform localization in invadosome rosettes, similar to that of the full-length myo1e (Fig. 4E). TH1 domain expressed separately exhibited a largely diffuse localization (Supplementary Fig. 1B). Thus, the addition of the lipid-binding TH1 domain to the proline-rich TH2 domain was sufficient for appropriate targeting of myo1e to newly forming invadosomes at the periphery of expanding rosettes. This suggests that although the TH2 domain acts as the initial localization signal for myo1e recruitment to invadosomes, the TH1 domain serves a functional purpose, potentially linking invadosome formation to the plasma membrane.

Since the proline-rich TH2 domain may potentially interact with the SH3 domain of myo1e, inducing oligomerization of myo1e, we coexpressed the GFP-tagged TH2 domain with the full-length myo1e tagged with mApple. We observed a striking difference between the localization of the TH2 domain and the full-length myo1e at invadosome rosettes (Fig. 4F), with the full-length myo1e enriched at the periphery and the TH2 domain uniformly distributed throughout the rosette. Thus, the recruitment of the myo1e TH2 construct to invadosome rosettes does not appear to be driven by oligomerization with the endogenous myo1e, since TH2 domain localization is distinct from that of the full-length myo1e.

To determine whether the differences in distribution of the various myo1e constructs throughout the rosette may be attributed to differences in their dynamics and turnover, FRAP analysis was performed to examine the rate of turnover of the GFP-tagged full-length myo1e, the TH1TH2 construct, and the TH2 domain (Supplementary Fig. 2). The goal of this experiment was to test whether the TH2 domain is unable to leave “older” invadosomes to relocate to the sites of new invadosome formation. By performing the FRAP analysis, we found that the full-length myo1e and TH1TH2 constructs showed similar dynamics within the invadosome rosettes, while the construct consisting of just the TH2 domain was much more dynamic and exchanged more rapidly. This suggests that the enrichment of the TH1TH2 construct and the full-length myo1e at the periphery of the rosette may be attributed to specific interactions targeting these proteins to the rosette periphery, rather than a delay in the detachment of the TH2 domain from older invadosomes.

Dominant-negative inhibition of myo1e results in mislocalization of newly forming invadosomes

To determine how myo1e activity affects invadosome rosette dynamics, as well as new invadosome formation, we observed rosette expansion in vanadate-treated cells over a longer time period. While many of the rosettes shown in Figs. 3 and 4 were observed for 1–2 min, for the time course of rosette expansion (Fig. 5) we observed each cell for at least 7 minutes, beginning at 10–15 min after vanadate addition. The time course observations were performed on cells expressing full-length myo1e or myo1e tail. The tail domain has been shown to act as a dominant-negative inhibitor of endogenous myo1e [2], presumably by competing with the endogenous myo1e for its binding partners. The cells for the time-course observation were selected based on two criteria: expression of both GFP- and mCherry-labeled constructs and the presence of a rosette of any size.

Invadosome rosettes were classified into four categories based on their fates. The rosette fates were categorized as fast expansion, slow expansion, steady state or collapse (Fig. 5A–D). With fast expansion, the rosette diameter changed very rapidly, so that

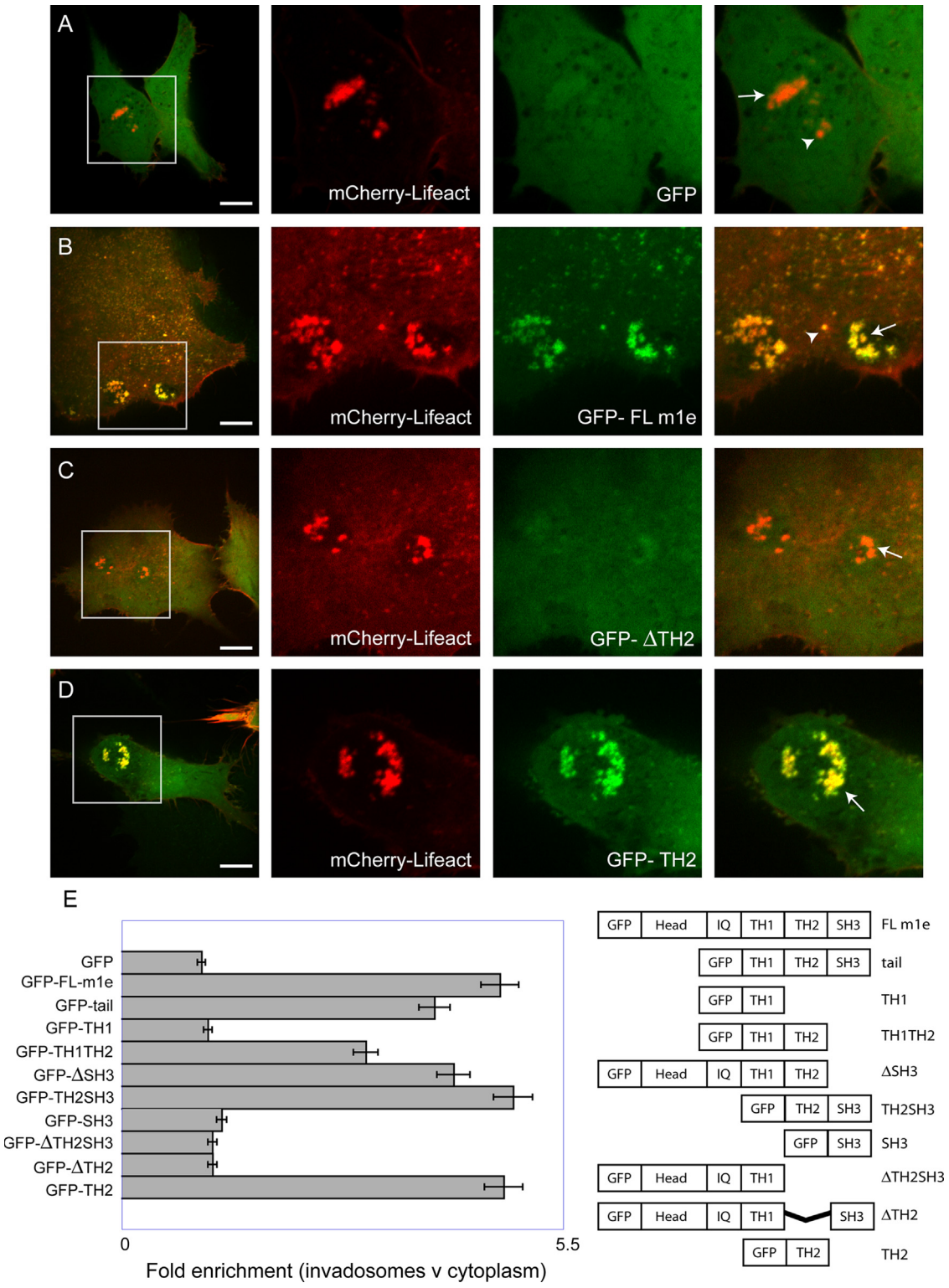

Fig. 2 – The TH2 domain of myo1e is necessary and sufficient for myo1e localization to invadosomes. RSV-transformed BHK-21 cells were transfected with GFP-tagged myo1e constructs along with mCherry-tagged Lifeact. (A) As a negative control, GFP was coexpressed with Lifeact. Lifeact was enriched at invadosomes clusters, while GFP fluorescence in invadosomes was just slightly over the cytoplasmic background. (B) Full-length myo1e tagged with GFP (GFP-FL myo1e) localized to invadosome clusters (arrows) and individual invadosomes (arrowheads), showing colocalization with actin. (C) Deletion of the proline-rich TH2 domain of myo1e significantly decreased the localization of myo1e to invadosome clusters. (D) The TH2 domain of myo1e localized to invadosome clusters, colocalizing with actin. (E) Graphical representation of the extent of construct localization to invadosome clusters, determined by calculating the fold enrichment of each construct at invadosome clusters relative to the cytoplasm as the ratio of mean fluorescence intensities. For each construct, at least 4 cells were analyzed. Error bars represent standard deviation. A schematic diagram of the constructs is shown on the right. Localization of the constructs not shown in this figure can be seen in Supplementary Fig. 1. In figures A–D, each inset shows invadosomes in a 30 by 30 μm square. Scale bars, 10 μm.

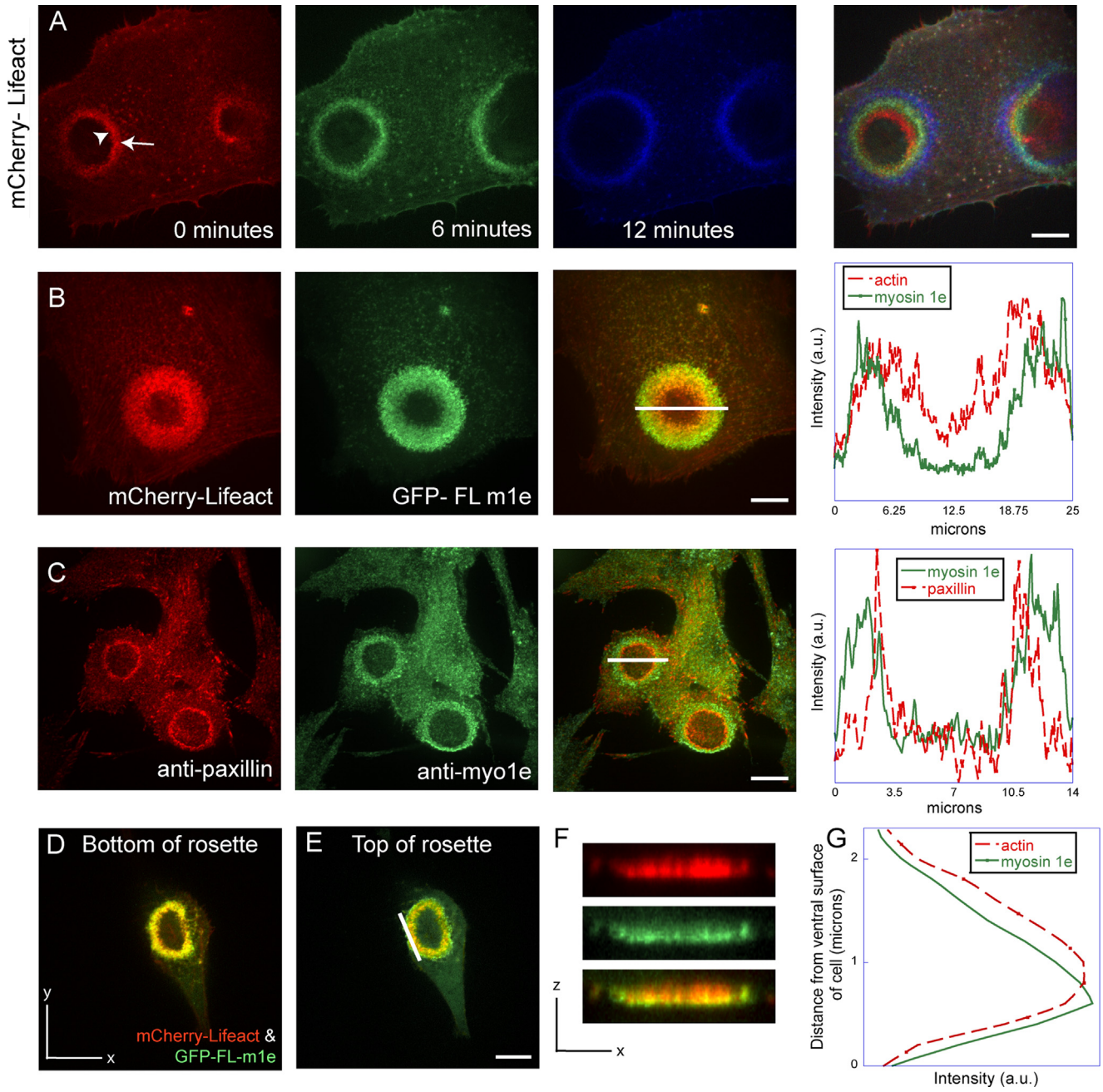

Fig. 3 – Myo1e localizes to the leading edge of expanding invadosome rosettes and precedes recruitment of actin and paxillin. (A) An example of invadosome rosette expansion upon vanadate treatment in RSV-transformed BHK-21 cells expressing mCherry-Lifeact. Over the course of 12 min (with time 0 corresponding to initiation of observation), we observed the enlargement of the invadosome rosette compared to its initial size (seen in red). Green represents rosette size after 6 min, and blue represents its size after 12 min. Arrowhead is labeling the inner rim of the rosette, while the arrow points to the outer rim of the rosette. (B) Myo1e localization relative to actin (labeled with Lifeact) in the expanding invadosome rosette observed in live cells. Myo1e was localized closer to the outer edge of the expanding rosette than actin. This was observed in 30 out of 30 cells examined. (C) Myo1e localization relative to paxillin was observed in fixed cells using anti-paxillin and anti-myo1e antibodies. This was observed in 12 out of 12 cells examined. In figures B and C, the line spanning the rosette represents a 20 pixel wide selection used to measure relative fluorescent intensity, which is plotted on the right. (D–F) Localization of myo1e and actin in Z-series of confocal images of expanding invadosome rosettes. Cells expressing myo1e and Lifeact show myo1e localizing to the ventral and lateral surfaces of invadosome rosettes. (F) Shows an X–Z projection of the Z-series. (G) The graph was generated using a linear selection (white line in E) and measuring mean fluorescence intensity for each z position within the stack. Scale bars, 10 μm.

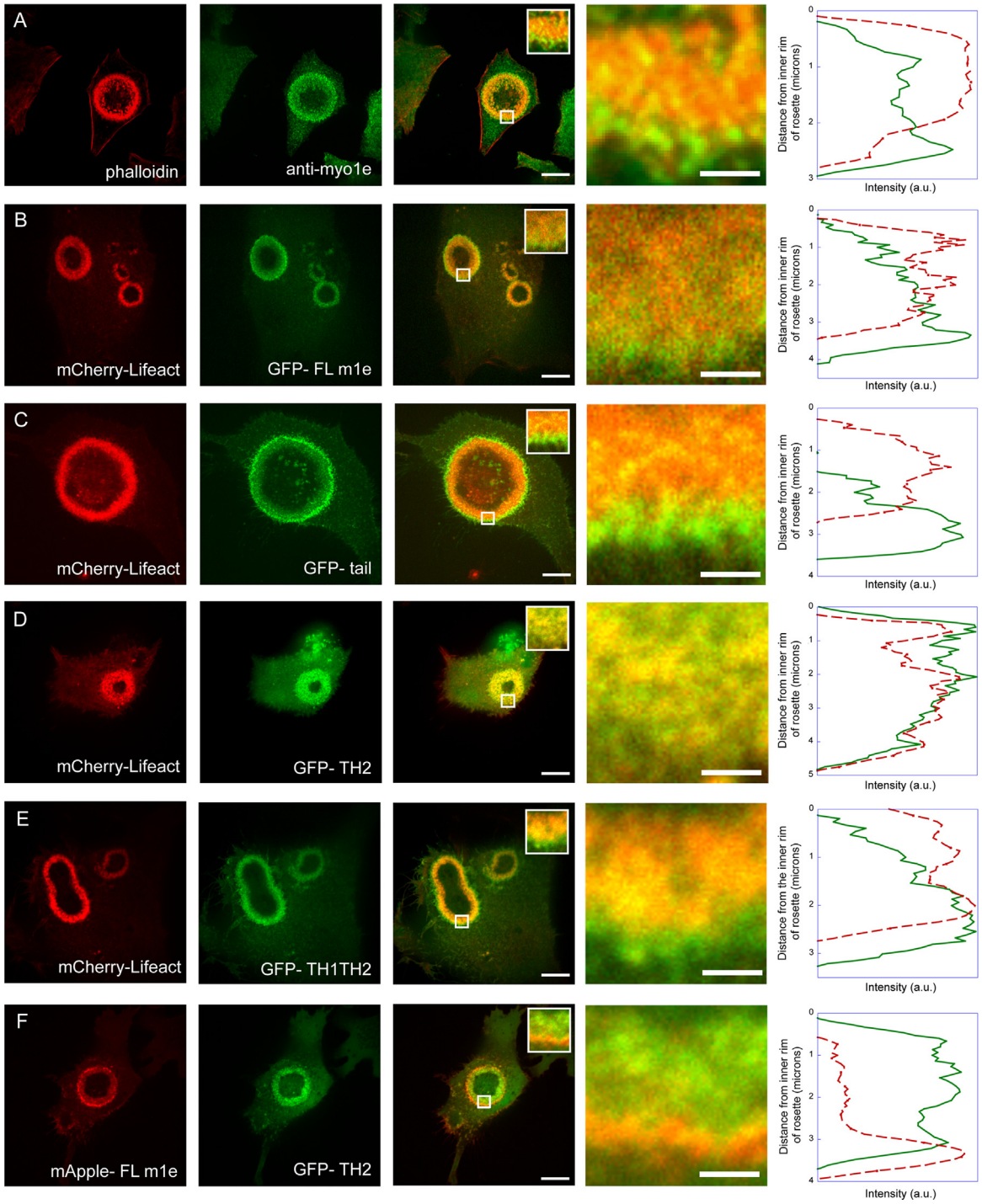

Fig. 4 – Localization of myo1e to the periphery of expanding invadosome rosettes requires TH1-dependent interactions with the plasma membrane. (A) RSV-BHK-21 cells were treated with vanadate, fixed, and stained with anti-myo1e antibody and phalloidin. Myo1e was enriched at the outer edge of the rosette. This was observed in 12 out of 12 cells examined. (B) GFP-tagged full length myo1e and (C) GFP-tagged myo1e tail were enriched at the periphery of the expanding rosette relative to mCherry-Lifeact. This was observed in 15 out of 16 cells expressing tail domain. (D) The TH2 domain of myo1e tagged with GFP colocalized with mCherry-Lifeact in vanadate-treated cells. This was observed in 11 out of 12 cells examined. (E) A GFP-tagged construct containing the TH1 and TH2 domains of myo1e coexpressed with mCherry-Lifeact localized to the periphery of the rosette in vanadate-treated cells. This was observed in 11 out of 11 cells examined. (F) The TH2 domain of myo1e tagged with GFP was coexpressed with mCherry-myo1e. The two proteins showed distinct localization patterns, with the full-length myo1e enriched at the periphery and the TH2 evenly distributed within the rosette. This was observed in 2 out of 2 cells examined. All insets represent enlargements of the 1.75 by 1.75 μm square regions indicated by the white squares in each of the merged images. The insets were used to measure mean fluorescence intensity values for all pixels with the same *Y* position (from the inner to the outer boundary of the rosette), and the results were plotted on the right. Peripheral enrichment of the endogenous myo1e (A) and the myo1e, tail, and TH1–TH2 constructs (B, C, E) can be observed as a green outline around the orange rosette. Scale bar, 10 μm. Inset scale bar, 0.5 μm.

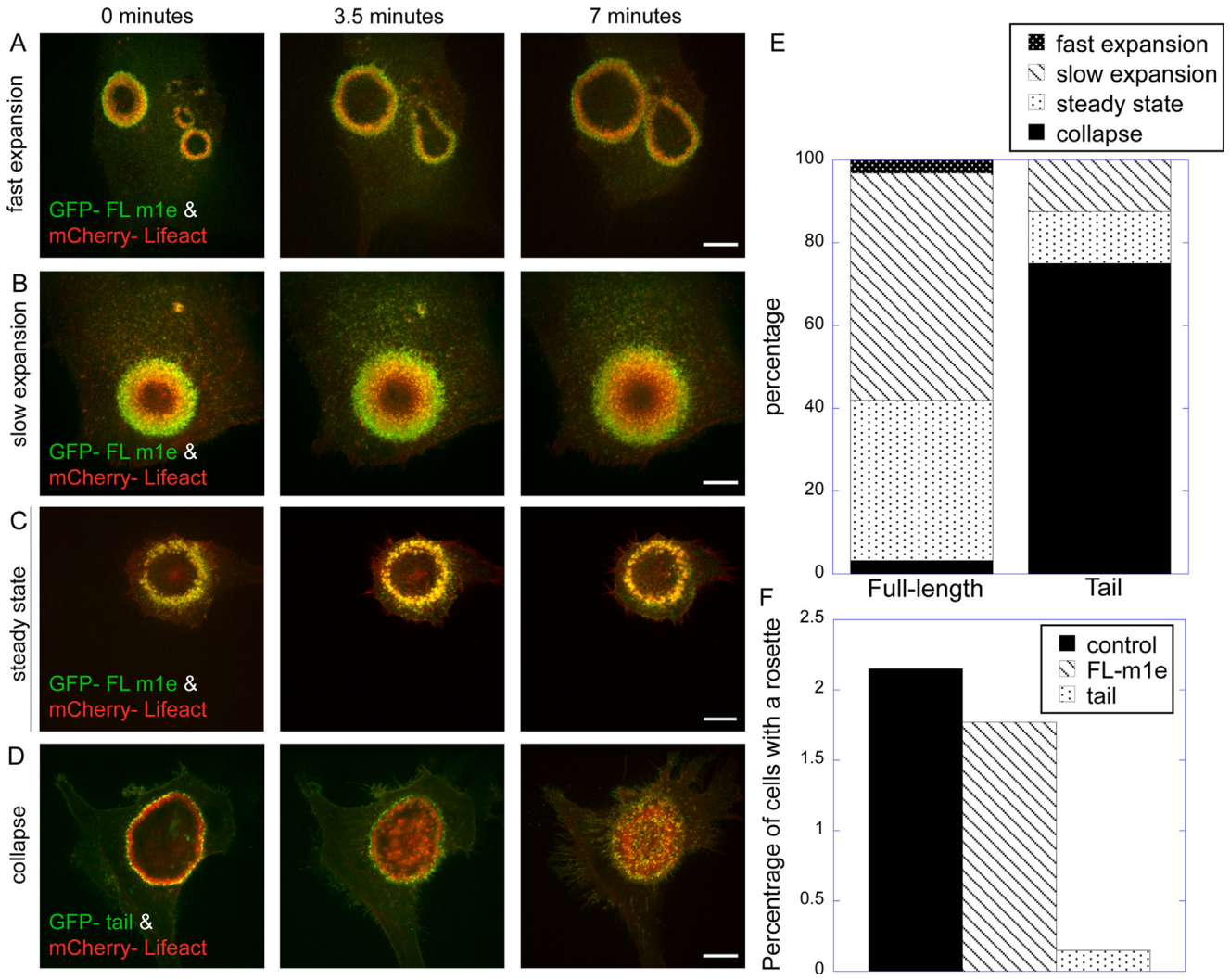

Fig. 5 – Dominant-negative inhibition of myo1e results in mislocalization of newly forming invadosomes. (A–D) Examples of invadosome rosette behavior over 7 min. Represented are fast expansion, slow expansion, steady state and collapse, which we defined as either a decrease in the size of the rosette or filling in of the center of the rosette with invadosome. Scale bar, 10 μm. (E) Cells expressing either full-length myo1e or myo1e tail myo1e were placed into one of the four categories described above. For the full-length myo1e, $n=31$, and for the myo1e tail, $n=21$. Quantities are displayed as percentages. (F) Cells expressing GFP-tagged constructs corresponding to the full-length myo1e or myo1e tail were treated with vanadate for 15 min, fixed, stained with phalloidin, and analyzed for the presence of invadosome rosettes. The number of GFP-expressing cells having rosettes was scored and expressed as a percentage of all GFP-expressing cells. Control cells represent untransfected, vanadate-treated cells (% of untransfected cells forming rosettes is displayed). $N=1300$ for each of the three groups.

there was no overlap of the rosette outlines at 0 and 3.5 min of observation. Collapse was defined as either a decrease in the size of the rosette, or "filling in" of the center of the rosette, which does not typically contain invadosomes, creating a solid circle of invadosomes rather than a ring. In over 90% of cells expressing full-length myo1e, rosettes either expanded or remained the same size (Fig. 5E). While the rapid expansion of the rosettes was observed in a relatively small percentage of cells (Fig. 5E), many cells expressing myo1e contained very large rosettes at 15–30 min post-treatment, suggesting that the expansion was occurring so rapidly that we were not always able to capture the process of rosette enlargement. Cells with rapidly expanding rosettes may be underrepresented in our analysis, as they may appear to be at a steady state following the initial expansion.

In contrast to the cells expressing full-length myo1e, 70% of the rosettes in cells expressing the dominant-negative tail construct collapsed (Fig. 5E). This suggests that the function of myo1e in invadosomes is essential for rosette expansion and/or for proper organization of the rosettes. In support of this hypothesis, cells expressing myo1e tail construct were less likely to form invadosome rosettes than cells expressing the full length myo1e construct (Fig. 5F). Thus, myo1e may play an important function in correctly targeting new invadosome formation to the plasma membrane surrounding the periphery of the rosette. Furthermore, the motor domain of myo1e appears to be necessary for invadosome rosette formation, since overexpression of the tail construct lacking the motor domain disrupts formation of rosettes.

Discussion

In this study, we used RSV-transformed BHK-21 fibroblasts, which readily form invadosomes and can be manipulated to induce a rapid expansion of invadosome rosettes, to examine the role of myo1e in invadosomes. Analysis of individual invadosomes showed that myo1e localized to their actin-rich core. Myo1e was surrounded by a ring of paxillin, and myo1e-rich areas coincided with the sites of matrix degradation, indicating that myo1e is a bona fide component of the invadosome core (Fig. 1). These observations are in line with the proteomic studies that identified myo1e as a component of the integrin adhesome [8] and macrophage podosomes [28]. Since myo1e enrichment in integrin-based adhesion complexes was not affected by the inhibition of myosin II [8], myo1e is unlikely to represent a component of large focal adhesions, whose formation depends on myosin II-mediated contractility. Indeed, in RSV-transformed BHK-21 cells myo1e was primarily enriched in invadosomes but not in focal adhesions. Upon vanadate treatment of RSV-transformed BHK-21 cells, myo1e became enriched at the newly forming invadosomes at the leading edge of expanding rosettes, where it preceded recruitment of both actin filament marker Lifeact and paxillin (Fig. 3).

Mapping of the invadosome-targeting regions on myo1e revealed that the proline-rich TH2 domain was both necessary and sufficient for localization to individual invadosomes and invadosome clusters in untreated cells (Fig. 2). However, TH2 domain alone was unable to preferentially localize to sites of new invadosome formation at the leading edge of expanding invadosome rosettes (Fig. 4). Unlike the full-length myo1e or the myo1e tail construct, TH2 domain alone was evenly distributed throughout the expanding rosette in vanadate-treated cells, mirroring the distribution of actin. The minimal myo1e construct exhibiting a distinct distribution to the periphery of the expanding rosette consisted of the membrane-binding TH1 domain and the proline-rich TH2 domain (Fig. 4). Thus, the proline-rich TH2 domain may interact with the SH3 domain-containing components of invadosomes to provide the initial signal for the myo1e localization, while the TH1 domain appears to be necessary to promote association of myo1e with the sites of active assembly of new invadosomes along the outer rim of the expanding invadosome rosette.

TH1 domain of myo1e is positively charged and has been shown to interact with anionic lipids, with some preference towards phosphoinositides with the phosphate in position 4 of the inositol ring (such as PtdIns(4,5)P_2 or PtdIns(3,4,5)P_3) [29]. Phosphoinositides that play important roles in invadosome formation include phosphatidylinositol 4,5-bisphosphate (PtdIns(4,5)P_2), phosphatidylinositol 3,4-bisphosphate (PtdIns(3,4)P_2), and PtdIns(3,4,5)P_3, [30,31]. Sequestration of phosphoinositides using appropriate PH domain expression or antibody injection blocks invadosome formation [30,31]. While the activity of many components of invadosomes, such as N-WASP and cortactin, can be regulated by phosphoinositides [32,33], the interaction between phosphoinositides and myo1e could serve as an additional means of modulating invadosome assembly and localization. The enrichment of myo1e along the outer surface of invadosome rosette could be driven by the interaction of TH1 domain with PtdIns(4,5)P_2, PtdIns(3,4)P_2, or PtdIns(3,4,5)P_3.

Among the markers of invadosomes whose localization in the expanding invadosome rosettes following vanadate treatment has been previously described (actin and paxillin), myo1e was unique in exhibiting a very strong preferential localization to the outer rim of expanding rosettes. Previously, paxillin, which is enriched at the inner rim of the rosette in vanadate-treated cells, was shown to be necessary for the disassembly of older invadosomes inside the rosette [18]. Additionally, in a study that highlighted the key role of integrin β1A subunit in formation of invadosome rosettes in Src-expressing mouse embryonic fibroblasts, integrin β1A was localized to the periphery of rosettes [34]. Thus, localization to the outer rim of the rosette may be characteristic of proteins that initiate new invadosome formation, while localization to the inner rim correlates with the role in invadosome disassembly.

We propose a model where myo1e is one of the proteins recruited to the newly forming invadosomes at the leading edge of the expanding rosette (Fig. 6A). The recruitment of myo1e occurs via interactions of the proline-rich TH2 with as yet unidentified invadosome components (Fig. 6B). In the dynamic model of invadosome rosette expansion, we propose that the positively charged TH1 domain of myo1e interacts with phosphoinositides in the plasma membrane to localize sites of new invadosome formation to the periphery of the rosette (Fig. 6B). The interaction of myo1e TH1 domain with the plasma membrane may help anchor myo1e to the plasma membrane and serve as an important regulator of invadosome formation. Myo1e may promote the expansion of invadosome rosettes by serving as a dynamic linker between the actin cytoskeleton and the plasma membrane. Invadosome formation is mediated by the Arp2/3 complex and therefore requires initial actin recruitment to provide mother filaments for new actin assembly; high concentration of myo1e at the periphery of the rosette may serve to anchor actin filaments to the plasma membrane and to establish an appropriate gradient of actin assembly within the rosette. In addition, myo1e may be able to recruit components of the actin polymerization machinery, such as the Arp2/3 activator N-WASP and its binding partner WIP [3]. Alternatively, myo1e motor activity along with its ability to interact with the plasma membrane may either help promote membrane deformation, which plays an important role in actin polymerization at invadosomes [35], or regulate vesicular trafficking to and from invadosomes. This is supported by myo1e interaction with dynamin 2, a GTPase that regulates actin assembly, membrane remodeling, and endocytosis. Similarly to myo1e, dynamin 2 localizes to invadosomes and is essential for invadosome assembly and turnover [20,36–38]. Furthermore, inhibition of dynamin activity using Dynasore inhibitor or depletion of dynamin interferes with matrix degradation [38,39]. Thus, both myo1e and its binding partner dynamin 2 may help regulate membrane curvature and actin assembly or direct vesicular trafficking at invadosomes. However, dynamin 2 localization in invadosome rosettes is more similar to that of paxillin than myo1e, with the enhanced accumulation along the inner rim of the rosette [38]; therefore, it is possible that dynamin 2 is more important for invadosome disassembly than for the formation of new invadosomes and performs functions distinct from myo1e.

Based on our model, we hypothesized that interfering with myo1e function may prevent correct localization of new invadosomes, and thus outward expansion of the rosette. Indeed,

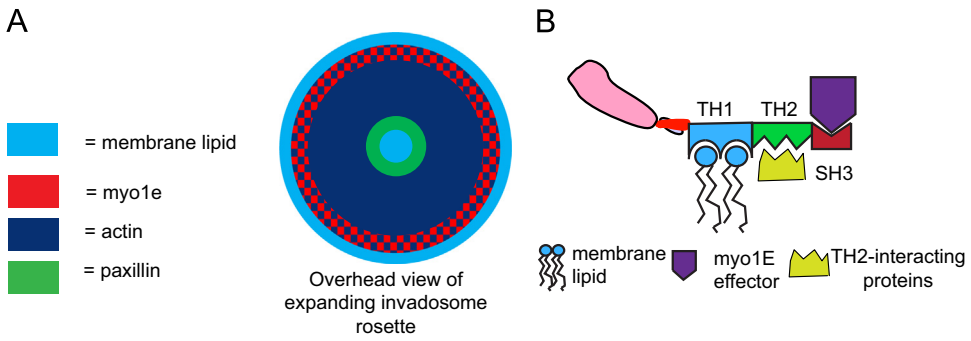

Fig. 6 – Model of invadosome rosette expansion. (A) Expansion of an invadosome rosette following vanadate treatment. Assembly of new invadosomes along the outer surface of the rosette leads to rosette expansion towards the cell periphery. Myo1e has more peripheral localization than other invadosome components, potentially serving as an adapter to bind invadosome components to the plasma membrane, thus allowing the expansion. (B) Predicted myo1e domain interactions. We propose a model where the TH2 domain is essential for the initial recruitment of myo1e through interactions with binding partners at invadosomes. Additionally, the TH1 domain binds membrane lipids, recruiting myo1e to the periphery of the invadosome rosette, and potentially allowing the rosette to expand through interactions with the plasma membrane. The SH3 domain may act as an effector domain, binding invadosome components containing proline-rich regions, such as WIP, N-WASP, or dynamin, and enhancing their recruitment and/or activation in invadosomes.

expression of the dominant-negative myo1e tail construct [2] prevented expansion of invadosome rosettes and induced rosette collapse in vanadate-treated cells (Fig. 5). While the expression of myo1e tail did not completely block formation of invadosome rosettes in response to vanadate, it appeared to change the directionality of expansion, thereby relocating sites of new invadosome formation towards the rosette center, and, concomitantly, reduced the number of cells with rosettes that could be found at a given time point. Presumably, the expression of the myo1e tail construct results in sequestration of the myo1e tail binding proteins, interfering with the normal functions of the endogenous myo1e. Expression of myosin tail domain constructs is often used to disrupt localization of myosin-binding proteins. For example, while myo1a tail domain is localized to the brush border in the intestinal epithelial cells, similarly to the endogenous myo1a, expression of the myo1a tail domain disrupts localization of the myo1a binding partner, sucrase–isomaltase, to the brush border [40]. Similarly, tail domain of myosin VI localizes to endocytic vesicles and inhibits endocytosis, probably by interfering with the functions of the endogenous myosin VI [41]. Thus, our observations suggest that myo1e role in invadosome rosette organization requires the presence of the motor domain, and that the expression of the tail construct lacking the motor domain disrupts invadosome rosette expansion.

Our findings identify myo1e as an invadosome core component that contributes to invadosome rosette formation and expansion in RSV-transformed BHK cells. Future studies will need to examine the role of myo1e in invadosome assembly and matrix degradation in other cell types where myo1e localizes to invadosomes (for example, MDA MB-231 breast cancer cells, unpublished observations). We propose that during the assembly of new invadosomes myo1e may be acting as a scaffold to recruit invadosome components to the plasma membrane and/or may be contributing to vesicular trafficking to the sites of assembly of new invadosomes.

Conflict of interest

None

Acknowledgments

This work was supported by the NIH award 1R01DK083345 to MK. The sponsor was not involved in study design, data collection, data interpretation, or the decision to publish the study. Myo1e construct corresponding to TH2 domain was provided by J. Bi. We are grateful to the members of Krendel lab and to J. Amack, S. Blystone, D. Pruyne, C. Turner, and V. Sirotkin for critical discussion of the manuscript, to N. Deakin and P. Calvert for advice on FRAP analysis, and to C. Pellenz and S. Chase for technical help.

Appendix A. Supporting information

Supplementary data associated with this article can be found in the online version at http://dx.doi.org/10.1016/j.yexcr.2014.01.015.

REFERENCES

[1] R.E. McConnell, M.J. Tyska, Leveraging the membrane – cytoskeleton interface with myosin-1, Trends Cell Biol. 20 (2010) 418–426.
[2] M. Krendel, E.K. Osterweil, M.S. Mooseker, Myosin 1E interacts with synaptojanin-1 and dynamin and is involved in endocytosis, FEBS Lett. 581 (2007) 644–650.
[3] J. Cheng, A. Grassart, D.G. Drubin, Myosin 1E coordinates actin assembly and cargo trafficking during clathrin-mediated endocytosis, Mol. Biol. Cell 23 (2012) 2891–2904.
[4] M. Krendel, S.V. Kim, T. Willinger, T. Wang, M. Kashgarian, R.A. Flavell, M.S. Mooseker, Disruption of Myosin 1e promotes podocyte injury, J. Am. Soc. Nephrol. 20 (2009) 86–94.
[5] S.E. Chase, C.V. Encina, L.R. Stolzenburg, A.H. Tatum, L.B. Holzman, M. Krendel, Podocyte-specific knockout of myosin 1e disrupts glomerular filtration, Am. J. Physiol. Renal. Physiol. 303 (2012) F1099–1106.
[6] J. Bi, S.E. Chase, C.D. Pellenz, H. Kurihara, A.S. Fanning, M. Krendel, Myosin 1e is a component of the glomerular slit diaphragm complex that regulates actin reorganization during

cell–cell contact formation in podocytes, Am. J. Physiol. Renal. Physiol. 305 (2013) F532–544.
[7] S.V. Kim, W.Z. Mehal, X. Dong, V. Heinrich, M. Pypaert, I. Mellman, M. Dembo, M.S. Mooseker, D. Wu, R.A. Flavell, Modulation of cell adhesion and motility in the immune system by Myo1f, Science 314 (2006) 136–139.
[8] H.B. Schiller, C.C. Friedel, C. Boulegue, R. Fassler, Quantitative proteomics of the integrin adhesome show a myosin II-dependent recruitment of LIM domain proteins, EMBO Rep. 12 (2011) 259–266.
[9] D.A. Murphy, S.A. Courtneidge, The 'ins' and 'outs' of podosomes and invadopodia: characteristics, formation and function, Nat. Rev. Mol. Cell Biol. 12 (2011) 413–426.
[10] S. Linder, C. Wiesner, M. Himmel, Degrading devices: invadosomes in proteolytic cell invasion, Annu. Rev. Cell Dev. Biol. 27 (2011) 185–211.
[11] H. Sibony-Benyamini, H. Gil-Henn, Invadopodia: the leading force, Eur. J. Cell Biol. 91 (2012) 896–901.
[12] G. Tarone, D. Cirillo, F.G. Giancotti, P.M. Comoglio, P.C. Marchisio, Rous sarcoma virus-transformed fibroblasts adhere primarily at discrete protrusions of the ventral membrane called podosomes, Exp. Cell Res. 159 (1985) 141–157.
[13] K.M. Branch, D. Hoshino, A.M. Weaver, Adhesion rings surround invadopodia and promote maturation, Biol. Open 1 (2012) 711–722.
[14] L.R. Boateng, A. Huttenlocher, Spatiotemporal regulation of Src and its substrates at invadosomes, Eur. J. Cell Biol. 91 (2012) 878–888.
[15] J.J. Bravo-Cordero, L. Hodgson, J. Condeelis, Directed cell invasion and migration during metastasis, Curr. Opin. Cell Biol. 24 (2012) 277–283.
[16] A.M. Weaver, Invadopodia: specialized cell structures for cancer invasion, Clin. Exp. Metastasis 23 (2006) 97–105.
[17] H. Yamaguchi, J. Wyckoff, J. Condeelis, Cell migration in tumors, Curr. Opin. Cell Biol. 17 (2005) 559–564.
[18] C. Badowski, G. Pawlak, A. Grichine, A. Chabadel, C. Oddou, P. Jurdic, M. Pfaff, C. Albiges-Rizo, M.R. Block, Paxillin phosphorylation controls invadopodia/podosomes spatiotemporal organization, Mol. Biol. Cell 19 (2008) 633–645.
[19] O. Destaing, F. Saltel, J.C. Geminard, P. Jurdic, F. Bard, Podosomes display actin turnover and dynamic self-organization in osteoclasts expressing actin-green fluorescent protein, Mol. Biol. Cell 14 (2003) 407–416.
[20] G.C. Ochoa, V.I. Slepnev, L. Neff, N. Ringstad, K. Takei, L. Daniell, W. Kim, H. Cao, M. McNiven, R. Baron, P.D.e. Camilli, A functional link between dynamin and the actin cytoskeleton at podosomes, J. Cell Biol. 150 (2000) 377–389.
[21] M.J. Taylor, D. Perrais, C.J. Merrifield, A high precision survey of the molecular dynamics of mammalian clathrin-mediated endocytosis, PLoS Biol. 9 (2011) e1000604.
[22] J.F. Skowron, W.M. Bement, M.S. Mooseker, Human brush border myosin-I and myosin-Ic expression in human intestine and Caco-2BBe cells, Cell Motil. Cytoskeleton 41 (1998) 308–324.
[23] J. Pignatelli, D.A. Tumbarello, R.P. Schmidt, C.E. Turner, Hic-5 promotes invadopodia formation and invasion during TGF-beta-induced epithelial-mesenchymal transition, J. Cell Biol. 197 (2012) 421–437.
[24] J.A. Gordon, Use of vanadate as protein-phosphotyrosine phosphatase inhibitor, Methods Enzymol. 201 (1991) 477–482.
[25] J. Riedl, A.H. Crevenna, K. Kessenbrock, J.H. Yu, D. Neukirchen, M. Bista, F. Bradke, D. Jenne, T.A. Holak, Z. Werb, M. Sixt, R. Wedlich-Soldner, Lifeact: a versatile marker to visualize F-actin, Nat. Methods 5 (2008) 605–607.
[26] J.N. Mazerik, M.J. Tyska, Myosin-1A targets to microvilli using multiple membrane binding motifs in the tail homology 1 (TH1) domain, J. Biol. Chem. 287 (2012) 13104–13115.
[27] P.C. Marchisio, N. D'Urso, P.M. Comoglio, F.G. Giancotti, G. Tarone, Vanadate-treated baby hamster kidney fibroblasts show cytoskeleton and adhesion patterns similar to their Rous sarcoma virus-transformed counterparts, J. Cell Biochem. 37 (1988) 151–159.
[28] P. Cervero, M. Himmel, M. Kruger, S. Linder, Proteomic analysis of podosome fractions from macrophages reveals similarities to spreading initiation centres, Eur. J. Cell Biol. 91 (2012) 908–922.
[29] E.A. Feeser, C.M. Ignacio, M. Krendel, E.M. Ostap, Myo1e binds anionic phospholipids with high affinity, Biochemistry 49 (2010) 9353–9360.
[30] H. Yamaguchi, S. Yoshida, E. Muroi, M. Kawamura, Z. Kouchi, Y. Nakamura, R. Sakai, K. Fukami, Phosphatidylinositol 4,5-bisphosphate and PIP5-kinase Ialpha are required for invadopodia formation in human breast cancer cells, Cancer Sci. 101 (2010) 1632–1638.
[31] T. Oikawa, T. Itoh, T. Takenawa, Sequential signals toward podosome formation in NIH-src cells, J. Cell Biol. 182 (2008) 157–169.
[32] R. Rohatgi, H.Y. Ho, M.W. Kirschner, Mechanism of N-WASP activation by CDC42 and phosphatidylinositol 4, 5-bisphosphate, J. Cell Biol. 150 (2000) 1299–1310.
[33] H. He, T. Watanabe, X. Zhan, C. Huang, E. Schuuring, K. Fukami, T. Takenawa, C.C. Kumar, R.J. Simpson, H. Maruta, Role of phosphatidylinositol 4,5-bisphosphate in Ras/Rac-induced disruption of the cortactin-actomyosin II complex and malignant transformation, Mol. Cell Biol. 18 (1998) 3829–3837.
[34] O. Destaing, E. Planus, D. Bouvard, C. Oddou, C. Badowski, V. Bossy, A. Raducanu, B. Fourcade, C. Albiges-Rizo, M.R. Block, Beta1A integrin is a master regulator of invadosome organization and function, Mol. Biol. Cell 21 (2010) 4108–4119.
[35] C. Albiges-Rizo, O. Destaing, B. Fourcade, E. Planus, M.R. Block, Actin machinery and mechanosensitivity in invadopodia, podosomes and focal adhesions, J. Cell Sci. 122 (2009) 3037–3049.
[36] M.A. McNiven, M. Baldassarre, R. Buccione, The role of dynamin in the assembly and function of podosomes and invadopodia, Front. Biosci. 9 (2004) 1944–1953.
[37] A. Bruzzaniti, L. Neff, A. Sanjay, W.C. Horne, P. De Camilli, R. Baron, Dynamin forms a Src kinase-sensitive complex with Cbl and regulates podosomes and osteoclast activity, Mol. Biol. Cell 16 (2005) 3301–3313.
[38] O. Destaing, S.M. Ferguson, A. Grichine, C. Oddou, P. De Camilli, C. Albiges-Rizo, R. Baron, Essential function of dynamin in the invasive properties and actin architecture of v-Src induced podosomes/invadosomes, PLoS One 8 (2013) e77956.
[39] A. Watanabe, D. Hoshino, N. Koshikawa, M. Seiki, T. Suzuki, K. Ichikawa, Critical role of transient activity of MT1-MMP for ECM degradation in invadopodia, PLoS Comput. Biol. 9 (2013) e1003086.
[40] M.J. Tyska, M.S. Mooseker, A role for myosin-1A in the localization of a brush border disaccharidase, J. Cell Biol. 165 (2004) 395–405.
[41] F. Buss, S.D. Arden, M. Lindsay, J.P. Luzio, J. Kendrick-Jones, Myosin VI isoform localized to clathrin-coated vesicles with a role in clathrin-mediated endocytosis, EMBO J. 20 (2001) 3676–3684.